Colossal enhancement of the magnetic dipole moment by exploiting lattice coupling in metasurfaces

ASO RAHIMZADEGAN[1,*], RASOUL ALAEE[1,2], THEODOSIOS D. KARAMANOS[1], ROBERT W. BOYD[2], AND CARSTEN ROCKSTUHL[1,3]

[1]*Karlsruhe Institute of Technology, Institute of Theoretical Solid State Physics, Wolfgang-Gaede-Str. 1, D-76131 Karlsruhe, Germany*
[2]*Department of Physics, University of Ottawa, Ottawa, ON K1N 6N5, Canada*
[3]*Institute of Nanotechnology, Karlsruhe Institute of Technology, 76021 Karlsruhe, Germany*
Corresponding author: aso.rahimzadegan@kit.edu

An artificial magnetic response is not only intellectually intriguing but also key to multiple applications. While previously suitably structured metallic particles and high-permittivity dielectric particles were used for this purpose, here, we highlight the possibility to exploit lattice effects to significantly enhance an intrinsically weak magnetic dipole moment of a periodically arranged scatterer. We identify the effective magnetic dipole moment as it is modulated by the lattice and coupled to other electromagnetic multipole moments the scatterer can sustain. Besides a more abstract consideration on the base of parametrized Mie coefficients to study the theoretical upper limit, we present an actual particle that shows an enhancement of the magnetic dipole moment by 100 with respect to what is attainable as a maximal value for an isolated particle. © 2022 Optical Society of America

---

1. INTRODUCTION

In recent years, structuring natural materials have enabled the control of their optical response in unprecedented ways [1–3][1]. Based on the gained insights, disruptive means emerged to mold the flow of light. Examples would be nanostructured metals with which light can be localized in deep-subwavelengths spatial domains by exploiting surface plasmon polaritons [4–6]. Another example are photonic crystals, i.e., dielectric materials periodically structured on length scales comparable to the wavelength that can suppress the propagation of light in selected spectral regions [7–11]. Besides, refraction and diffraction can be tailored at will while controlling the dispersion relation of the permissible solutions to Maxwell's equations in photonic crystals [12]. But potentially most dramatic along these lines of research has been the notion of metamaterials [2, 3, 13–15]. Metamaterials are characterized by a subwavelength period and designed, primarily, to control the propagation of light as it would be possible with a homogeneous medium characterized by properties inaccessible with natural materials; or at least unavailable with its constituting materials. Research on metamaterials considered initially anisotropic dielectric properties at the effective level. This is called form birefringence [16, 17]. Later, research focused on chiral [18] or, slightly more general, bi-anisotropic materials [19–
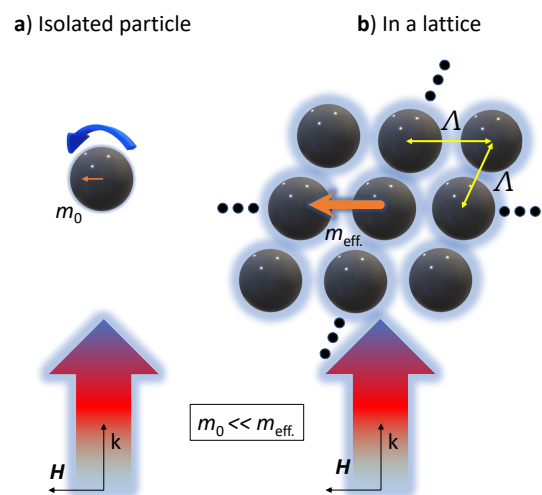
Fig. 1. An artistic impression of the article. b) A lattice can significantly enhance the magnetic response of a particle in comparison to a) when considering the particle as isolated.

---

[1]A notable contribution to this progress came from Costas M. Soukoulis and his team(s). We thank him for this inspiration and would like to wish him Happy Birthday on that occasion.

23]. But an artificial magnetism has triggered the largest share of excitement. No natural material at optical frequencies supports a magnetic response, and the permeability corresponds to that of vacuum [13, 14]. Therefore, in most textbooks, it is quite canonically stated that the relative permeability can be put to unity, and magnetic effects do not need to be considered. However, this is quite a self-imposed limitation. It was shown, a long time ago, that in the presence of magnetic media, many effects occur quite counter-intuitive at optical frequencies [24]. A game-changer has been the suggestion for a perfect lens made from a medium characterized by both negative permittivity and permeability [25]. Moreover, the notion of transformation optics, where permittivity and permeability are distributed suitably in space according to a receipt that came from considering light propagation in homogeneous and isotropic but curved spaces, liberated our way to think about the design of optical elements [26, 27]. All these possibilities were motivation to seek materials that offer an artificial magnetic response at some effective level. Nowadays, mostly two approaches are established.

The first approach relies on structuring metallic materials to some interrupted ring-shaped objects [28, 29]. The idea is always to let the external field induce a conduction current with a ring shape that gives rise to an induced magnetic dipole moment [30]. The interruption of the ring is necessary to drive the oscillation into resonance at an elevated frequency. Placing many of such artificial magnetic dipoles in an array allows observing at the effective level dispersion in the permeability [31]. Metallic structures have been advantageous to reach a deep sub-wavelength scale [32, 33]. Canonical elements have been split-ring resonators [34, 35] or cut-plate pairs [36], but many other structural elements can be equally envisioned. However, the use of metals is inevitably accompanied by dissipation. And the absorption of light often prevents the exploitation of the interesting dispersive effects. Even though this is not a fundamental obstacle, the mitigation of the absorption problem would have been great [37].

That, in turn, led to the second approach to observe an artificial magnetic response [38–40]. Specifically, already spheres made from a high index dielectric material sustain, in the form of Mie resonances, strong magnetic dipole moments that can be induced around some discrete frequencies. We can think of these magnetic dipole moments as a consequence of an induced displacement current instead of a conduction current in a metal. Balancing the electric and magnetic dipole moment so that they have the same polarizability in isotropic particles or suitably shaped dielectric discs gives rise to a Huygens' scatterer, which scatters light exclusively in the forward direction [41–46]. While operating in a spectral proximity to resonance, the phase of the light scattered in forward direction can be tuned almost in the entire range from 0 to 2π [47]. This scattering behavior opens unprecedented opportunities for applications when these particles are arranged to form an array.

While it has been to some extent already discussed in literature [48–50], we emphasize here in a systematic analysis a third mechanism with which a strong magnetic dipole moment in a structured material can be induced. We demonstrate that a rather small intrinsic magnetic dipole moment from an object can be significantly enhanced thanks to the lattice interaction. An artistic impression of that idea is shown in Fig. 1. For an object characterized by a magnetic dipole moment only, an enhancement as large as fourfold is observed in the array. A colossal enhancement by up to two orders of magnitude is witnessed when exploiting a re-normalization by the lattice interaction

thanks to an electric quadrupole moment sustained in the particle. Our work highlights the possibility of capitalizing on the lattice effect to tune the response from periodically arranged structured materials in a drastic manner.

The contribution is organized as follows. First, we derive the maximum magnetic dipole moment for an isolated isotropic scatterer. Next, utilizing a suitable parametrization of the optical response of isotropic particles known as the Mie angles, we systematically search for a lattice-induced enhancement of the induced magnetic dipole moment by a normally incident plane wave excitation. Afterward, we explore the lattice-induced coupling of the electric quadrupole moment of the individual particle to the magnetic dipole moment and its effect on the overall enhancement of the induced magnetic dipole moment. The colossal induced magnetic dipole moment occurs when the denominator of the expression describing the re-normalization of the magnetic dipolar polarizability in the lattice is close to zero. We provide the complete recipe to hit the sweet spots and identify the required Mie coefficients to provide two orders of overall magnitude enhancement. Developing upon that, and as a proof of principle, using a particle swarm optimization algorithm [51], we design a core-shell particle that satisfies the required Mie coefficients. Placing this particle in a lattice shows an enhancement of the magnetic dipole moment by two orders of magnitude. At the point of the colossal enhancement, the effective electric quadrupole moment is significantly enhanced as well. This simultaneous enhancement suppresses specific far-field effects, but the signatures in the near-field are pretty clear.

2. MULTIPOLAR ANALYSIS FORMULATION

We consider time-harmonic fields and assume their dependency according to $e^{-i\omega t}$. We start our discussion by expressing the induced Cartesian multipole moments in a particle up to quadrupolar order. These induced moments can be written as [52–54]

$$
\begin{bmatrix}
\mathbf{p}/\varepsilon \\
k\mathbf{Q}^{\mathrm{e}}/\left(\varepsilon\sqrt{60}\right) \\
i\eta\mathbf{m} \\
i\eta k\mathbf{Q}^{\mathrm{m}}/\sqrt{60}
\end{bmatrix}
= \frac{6\pi}{k^3}\widetilde{\widetilde{\alpha}}
\begin{bmatrix}
\mathbf{E}_1 \\
k^{-1}\sqrt{20/3}\,\mathbf{E}_2 \\
i\eta\mathbf{H}_1 \\
i\eta k^{-1}\sqrt{20/3}\,\mathbf{H}_2
\end{bmatrix}. \tag{1}
$$

The electric dipole ($\mathbf{p}$) and electric quadrupole ($\mathbf{Q}^{\mathrm{e}}$) moments and the electric field ($\mathbf{E}_1$) and its gradients ($\mathbf{E}_2$) as used in Eq. (1) are defined as [54–56]

$$
\mathbf{p} = [p_x\; p_y\; p_z]^T, \tag{2a}
$$

$$
\mathbf{Q}^{\mathrm{e}} = \begin{bmatrix} Q_{xy}^{\mathrm{e}} & Q_{yz}^{\mathrm{e}} & \sqrt{3}/2\,Q_{zz}^{\mathrm{e}} & Q_{xz}^{\mathrm{e}} & \left(Q_{xx}^{\mathrm{e}} - Q_{yy}^{\mathrm{e}}\right)/2 \end{bmatrix}^T, \tag{2b}
$$

and

$$
\mathbf{E}_1 = \begin{bmatrix} E_x & E_y & E_z \end{bmatrix}^T, \tag{3a}
$$

$$
\mathbf{E}_2 = \frac{1}{2\sqrt{3}}
\begin{bmatrix}
\partial_y E_x + \partial_x E_y \\
\partial_y E_z + \partial_z E_y \\
\sqrt{3}\,\partial_z E_z \\
\partial_x E_z + \partial_z E_x \\
\partial_x E_x - \partial_y E_y
\end{bmatrix}. \tag{3b}
$$

The magnetic multipole moments $\mathbf{m}$ and $\mathbf{Q}^m$ and the respective fields $\mathbf{H}_1$ and $\mathbf{H}_2$ are defined in a similar way as the case of Eq. (1) but multiplied with a prefactor $i\eta$. ε is the permittivity, and η is the impedance of the medium.

The properties of the object, whether considered isolated or placed along a lattice, can expressed up to quadrupolar order by the normalized polarizability tensor $\widetilde{\overline{\overline{\alpha}}}$. It can be written as,

$$
\widetilde{\overline{\overline{\alpha}}} = \begin{bmatrix}
\widetilde{\overline{\alpha}}_{11}^{ee} & \widetilde{\overline{\alpha}}_{12}^{ee} & \widetilde{\overline{\alpha}}_{11}^{em} & \widetilde{\overline{\alpha}}_{12}^{em} \\
\widetilde{\overline{\alpha}}_{21}^{ee} & \widetilde{\overline{\alpha}}_{22}^{ee} & \widetilde{\overline{\alpha}}_{21}^{em} & \widetilde{\overline{\alpha}}_{22}^{em} \\
\widetilde{\overline{\alpha}}_{11}^{me} & \widetilde{\overline{\alpha}}_{12}^{me} & \widetilde{\overline{\alpha}}_{11}^{mm} & \widetilde{\overline{\alpha}}_{12}^{mm} \\
\widetilde{\overline{\alpha}}_{21}^{me} & \widetilde{\overline{\alpha}}_{22}^{me} & \widetilde{\overline{\alpha}}_{21}^{mm} & \widetilde{\overline{\alpha}}_{22}^{mm}
\end{bmatrix},
\tag{4}
$$

with the sub- and superscripts being rather intuitive. Subscripts 1 and 2 refer to dipolar and quadrupolar contributions, while the superscripts e and m refer to electric and magnetic contributions, respectively. The polarizability can be defined as [54]

$$
\overline{\overline{\alpha}}_{jj'}^{vv'} = \frac{\sqrt{(2j+1)(2j'+1)}\pi}{k^j k^{j'} k} \widetilde{\overline{\overline{\alpha}}}
\tag{5}
$$

where $\{j, j'\} = \{1, 2\}$ and $\{v, v'\} = \{e, m\}$. The use of a normalized polarizability tensor simplifies the systematic search process significantly.

For an isolated isotropic particle, i.e. a particle with a spherical symmetry not placed in a lattice, the polarizability tensor is a diagonal matrix. This expresses the fact that multipolar fields of different order do not couple to each other. The diagonalized polarizability tensor at Eq. (4) simplifies to

$$
\widetilde{\overline{\overline{\alpha}}}_0 = \mathrm{Diag}\left(\widetilde{\alpha}_p, \widetilde{\alpha}_p, \widetilde{\alpha}_p, \widetilde{\alpha}_{Q^e}, \widetilde{\alpha}_{Q^e}, \widetilde{\alpha}_{Q^e}, \widetilde{\alpha}_{Q^e}, \widetilde{\alpha}_m, \widetilde{\alpha}_m, \widetilde{\alpha}_m, \widetilde{\alpha}_{Q^m}, \widetilde{\alpha}_{Q^m}, \widetilde{\alpha}_{Q^m}, \widetilde{\alpha}_{Q^m}\right).
\tag{6}
$$

where $\widetilde{\alpha}_p$ $(\widetilde{\alpha}_m)$, and $\widetilde{\alpha}_{Q^e}$ $(\widetilde{\alpha}_{Q^m})$ are the normalized electric (magnetic) dipole and quadrupole polarizability moments, respectively. For an isotropic particle, simple relations between the polarizability and the Mie coefficients of the particles exist, namely [47, 56]

$$
\widetilde{\alpha}_p = ia_1, \quad \widetilde{\alpha}_m = ib_1, \quad \widetilde{\alpha}_{Q^e} = ia_2, \quad \widetilde{\alpha}_{Q^m} = ib_2.
\tag{7}
$$

When arranging identical particles on a lattice, the normalized polarizability of the individual particle $\widetilde{\alpha}_0$, should in turn be re-written as a function of the lattice interaction. Consequently, the effective polarizability is calculated as [54, 57]

$$
\widetilde{\overline{\overline{\alpha}}}_{\text{eff.}}(\lambda) = \left[\overline{\overline{I}} - \widetilde{\overline{\overline{\alpha}}}_0(\lambda)\,\overline{\overline{C}}\left(\Lambda/\lambda, \hat{k}_{\text{inc.}}\right)\right]^{-1} \widetilde{\overline{\overline{\alpha}}}_0(\lambda)
\tag{8}
$$

where $\overline{\overline{C}}$ is the coupling lattice tensor [57–59], λ is the operating wavelength, Λ is the periodicity of the lattice, $\overline{\overline{I}}$ is a unity matrix, and $\hat{k}_{\text{inc.}}$ is the direction of incident plane wave excitation. We have included the arguments herein to emphasize that the lattice coupling tensor is a function of the normalized periodicity and the direction of the plane wave illumination. With such a lattice interaction, the polarizability entries on the diagonal get modified, but the appearance of non-diagonal elements is also worth mentioning. Therefore, placing the particle on a lattice changes the symmetry of the response. This change in symmetry is not surprising and can be explained from two perspectives. On the one hand, the particles arranged on a lattice do not obey the necessary isotropic, i.e., directional independent, response. On the other hand, we can note that the quadrupolar response from a particle in the lattice generates a scattered field that can drive the dipolar response in any other particle in the lattice. This

cross-coupling effectively causes an interaction that is otherwise forbidden for the isolated object. Both interaction channels can be exploited to effectively enhance, for example, the magnetic dipole moment, on which we concentrate in this contribution.

We discuss the modification to the polarizability of a particle if placed within a square lattice. The sample is illuminated at normal incidence (i.e., $\hat{k}_{\text{inc.}} = \hat{\mathbf{e}}_z$) with a linearly polarized plane wave. The response is polarization-independent and the same for either TE or TM polarization. Therefore, without losing generality, we choose in the following the TM polarization, i.e.,

$$
\begin{bmatrix} E_x & E_y & E_z \end{bmatrix}^T = E_0 e^{ikz} \begin{bmatrix} 1 & 0 & 0 \end{bmatrix}^T
\tag{9}
$$

where E_0 is the amplitude of the incident field.

This specific setting allows to write out explicitly the equations that express the induced multipole moment (Eq. (1)) while considering their re-normalization due to the lattice interaction (Eq. (8)), and the description of the particle using the Mie coefficient (Eq. (7)). The induced multipole moments in each particle up to quadrupolar order are, then, derived as [54]

$$
\begin{bmatrix}
p_x/\varepsilon \\
Q_{xz}^e/\varepsilon \\
\eta m_y \\
\eta Q_{yz}^m
\end{bmatrix}
=
\begin{bmatrix}
\frac{6\pi i}{k^3} a_{1,\text{mod.}}^{b_2} \\
\frac{-60\pi}{k^4} a_{2,\text{mod.}}^{b_1} \\
\frac{6\pi i}{k^3} b_{1,\text{mod.}}^{a_2} \\
\frac{-60\pi}{k^4} b_{2,\text{mod.}}^{a_1}
\end{bmatrix}
E_0.
\tag{10}
$$

The polarizabilities of the particles in these expressions depend on (a) the interaction among the same multipole moments in the lattice (i.e., modulation) and (b) the coupling with other multipole moments in the lattice. Note that not all multipole moments couple to each other. Indeed, each multipole moment is influenced by only one other multipole moment for up to quadrupolar order. The respective multipole moment is mentioned in the superscript. To be specific, electric (magnetic) dipole moments are coupled to magnetic (electric) quadrupole moments and vice versa. The as such dressed Mie coefficients are written as

$$
\frac{1}{a_{1,\text{mod.}}^{b_2}} = \frac{1 + C_{dQ}^2 b_{2,\text{mod.}} a_{1,\text{mod}}}{a_{1,\text{mod.}}\left(1 + i\sqrt{5/3}\,C_{dQ} b_{2,\text{mod.}}\right)},
\tag{11}
$$

$$
\frac{1}{b_{1,\text{mod.}}^{a_2}} = \frac{1 + C_{dQ}^2 a_{2,\text{mod.}} b_{1,\text{mod.}}}{b_{1,\text{mod.}}\left(1 + i\sqrt{5/3}\,C_{dQ} a_{2,\text{mod}}\right)},
\tag{12}
$$

$$
\frac{1}{a_{2,\text{mod.}}^{b_1}} = \frac{1 + C_{dQ}^2 b_{1,\text{mod.}} a_{2,\text{mod.}}}{a_{2,\text{mod.}}\left(1 + i\sqrt{3/5}\,C_{dQ} b_{1,\text{mod.}}\right)},
\tag{13}
$$

$$
\frac{1}{b_{2,\text{mod.}}^{a_1}} = \frac{1 + C_{dQ}^2 a_{1,\text{mod.}} b_{2,\text{mod.}}}{b_{2,\text{mod.}}\left(1 + i\sqrt{3/5}\,C_{dQ} a_{1,\text{mod.}}\right)},
\tag{14}
$$

where C_{dd}, C_{QQ}, C_{dQ} are dipole-dipole, quadrupole-quadrupole, and dipole-quadrupole coupling tensor elements [54]. The Mie coefficients that appear in these expressions on the right hand side are those that are modulated thanks to the coupling to

themselves in the lattice. They are explicitly written as

$$\frac{1}{a_{1,\text{mod.}}} = \frac{1}{a_1} - iC_{\text{dd}} \tag{15}$$

$$\frac{1}{b_{1,\text{mod.}}} = \frac{1}{b_1} - iC_{\text{dd}} \tag{16}$$

$$\frac{1}{a_{2,\text{mod.}}} = \frac{1}{a_2} - iC_{\text{QQ}} \tag{17}$$

$$\frac{1}{b_{2,\text{mod.}}} = \frac{1}{b_2} - iC_{\text{QQ}}. \tag{18}$$

Writing the above equations in such a manner has many advantages. First of all, we can immediately distinguish the impact of the lattice on the multipole moments of the same or different order. Moreover, the above equations hold for isolated particles outside a lattice when replacing the effective coupled Mie coefficients with the Mie coefficient of the individual particles. Or, in other words, all the coupling terms vanish. In the following, we concentrate on enhancing the magnetic dipole moment in the lattice with increasing complexity.

Before quantifying the enhancement, we have to set a stage concerning what can be reached for an isotropic, isolated, passive, and non-absorbing particle. The magnetic dipole moment induced in such a particle can be written as [60]

$$m_0 = \frac{6\pi i E_0}{\eta k^3} b_1 \tag{19}$$

where b_1 is the dipolar magnetic Mie coefficient. Note that we have drooped the y subscript for brevity since the excited magnetic moment will always point towards the y-axis with the TM illumination assumed. In the following, we wish to study the problem systematically. Any possible value the magnetic dipole Mie coefficient can take is, herein, parameterized using the so-called Mie angles θ_{Mj} [61–63]

$$b_j = \cos\theta_{Mj} \exp i\theta_{Mj}, \tag{20}$$

where $-\pi/2 \leq \theta_{Mj} \leq \pi/2$. An identical equation can be used to parameterize the electric Mie coefficients using the electric Mie angles θ_{Ej} in the parametrization instead. The maximal magnitude of the magnetic dipole moment is at resonance (i.e., $\theta_{M1} = 0$) and is equal to

$$m_{\text{max}} = \left| \frac{6\pi i E_0}{\eta k^3} \right| = \frac{6\pi E_0}{\eta k^3}. \tag{21}$$

This maximal value serves to normalize the possible response and constitutes a reference value to quantify the enhancement of the magnetic dipole moment inside a lattice. For completeness, the normalized magnetic dipole moment as a function of the Mie angle is illustrated in Fig. 2(a). Notice that the normalized magnetic dipole moment takes the value of one at resonance.

3. LATTICE MADE FROM A PARTICLE WITH ONLY A MAGNETIC DIPOLAR RESPONSE

The initial question is how much larger this magnetic dipole moment can be enhanced when placing the magnetic dipolar scatterer inside a lattice. The question can be answered by specifying the previously considered equations applicable to purely magnetic dipolar particles. Therefore, the induced magnetic dipole moment inside a square lattice array upon normal plane wave illuminations reads as

$$m_{\text{mod.}} = \frac{6\pi i E_0}{\eta k^3} b_{1,\text{mod.}} = \frac{6\pi i E_0}{\eta k^3} \frac{b_1}{1 - i\,b_1 C_{\text{dd}}}, \tag{22}$$
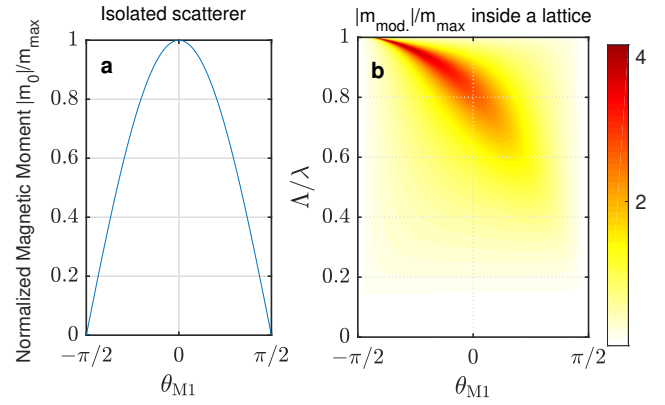
Fig. 2. Magnitude of the induced magnetic dipole moment normalized to the maximum induced magnetic dipole moment of an isolated scatterer in vacuum as a function of the magnetic dipole Mie coefficient angle for **a**) an isolated magnetic dipole and **b**) a magnetic dipole inside a lattice with a normalized periodicity of Λ/λ.

where the normalized modulated magnetic dipole moment is

$$\frac{m_{\text{mod.}}}{m_{\text{max}}} = \frac{i\,b_1}{1 - i\,b_1 C_{\text{dd}}}. \tag{23}$$

Any possible value of the magnetic dipole moment at a given operating wavelength now depends on only two parameters: the Mie angle, which parameterizes the response of the individual particle, and the periodicity of the lattice. The magnitude of the modulated normalized magnetic dipole moment is plotted in Fig. 2(b).

The maximal enhancement thanks to the lattice interaction is slightly more than four and occurs in a parameter region where the lattice is still sub-wavelength but very close to the diffraction zone. Using the conservation of energy relationships, it can be proven that the maximum value of the normalized magnetic dipole moment in such lattices can reach to a fundamental upper limit of $4\pi/3$ at the extreme point of $\Lambda = \lambda$. The polarizability of the individual particle has to be off-resonant. To be specific, the Mie angle can be translated to a frequency detuning [63]; a negative Mie angle suggests a frequency smaller than the resonance one, while a positive Mie angle suggests a frequency larger than the resonance one. The particle, therefore, has to be mainly operated below its resonance frequency. The lattice interaction drives the particle into a resonance, where it gets enhanced far beyond the value it can attain when placed outside the lattice. This is a usual behavior when observing the resonance from dipolar particles in the lattice, i.e., for larger periodicities, the lattice interaction shifts the resonance towards longer wavelengths and hence smaller frequencies. In the limiting case, albeit the resolution in the figure is slightly too small to recognize these details, the largest magnetic dipole moment occurs for a particle that has intrinsically a very weak magnetic dipole moment (i.e., the Mie angle is only slightly larger than $-\pi/2$) but arranged at a period nearly comparable to the wavelength and only slightly smaller.

The next question that we aim to answer in the following section concerns the possibility to enhance this magnetic dipole moment even stronger.
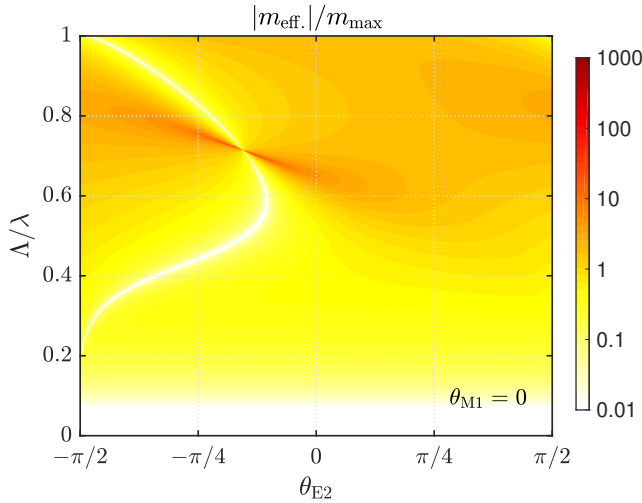
Fig. 3. The magnitude of the effective induced magnetic dipole moment $m_{\text{eff.}}$ of a scatterer with only magnetic dipole moment and electric quadrupole response normalized to the maximal possible magnetic dipole moment of an isolated scatterer in vacuum m_{max} as a function of the normalized periodicity Λ/λ and as a function of the Mie angle that parametrizes the electric quadrupolar Mie coefficient. The magnetic dipole Mie angle is kept fixed to the value necessary to induce a resonance in isolation, i.e. $\theta_{\text{M1}} = 0$.

4. LATTICE MADE FROM PARTICLES WITH A MAGNETIC DIPOLAR AND ELECTRIC QUADRUPOLAR RESPONSE

Considering Eq. (11), the multipole moment that couples to and re-normalizes the magnetic dipole moment, beside the modulation with the dipole-dipole lattice tensor element C_{dd}, is the electric quadrupole moment. Taking into account this interaction, the effectively induced magnetic dipole moment inside the square lattice can be explicitly written as

$$m_{\text{eff.}} = \frac{6\pi i E_0}{\eta k^3} b_{1,\text{mod.}}^{\widehat{a_2}} = \frac{6\pi i E_0}{\eta k^3} \frac{b_{1,\text{mod.}} \left(1 + i\sqrt{5/3}\, C_{\text{dQ}}\, a_{2,\text{mod.}}\right)}{1 + C_{\text{dQ}}^2\, a_{2,\text{mod.}}\, b_{1,\text{mod.}}}, \quad (24)$$

where $b_{1,\text{eff}}$ follows the expression given in Eq. (15). To explore the possible value the magnetic dipole moment can attain systematically, we utilize the Mie angles again to parametrize the possible Mie coefficients that an isotropic scatterer can attain and, afterward, derive the possible magnetic moments inside a square lattice. Please note that there are now three degrees of freedom: the Mie angle parametrizing the magnetic dipole moment θ_{M1}, the Mie angle parametrizing the electric quadrupole moment θ_{E2}, and the normalized periodicity of the square lattice Λ/λ.

For illustrative purposes, Fig. 3 shows the normalized magnetic dipole moment as a function of the Mie angle parametrizing the electric quadrupole Mie coefficient of the individual particle and the normalized periodicity of the lattice. Here, the Mie angle parameterizing the magnetic dipole moment was kept fixed to zero, i.e., the particle is on magnetic dipole resonance if place isolated.

A colossal enhancement of the magnetic dipole moment is seen in Fig. 3 for some sweep spots. This colossal enhancement occurs whenever the denominator for the effective coupled mag-
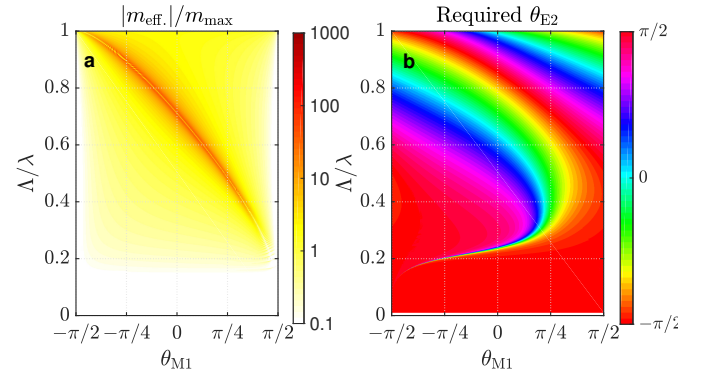
Fig. 4. a) The maximal possible enhancement of the magnetic dipole moment for a scatterer with an intrinsic magnetic dipole and electric quadrupole response inside a lattice with periodicity of Λ as a function of the Mie angle that parametrizes the magnetic dipolar Mie coefficient. b) The required Mie angle for the electric quadrupole Mie coefficient required to attain the maximal value.

netic dipole Mie coefficient is close to zero in Eq. (24). Please note, the denominator does not go through zero strictly but gets very close. When comparing the two dependencies, we notice that the re-normalization thanks to the electric quadrupolar response is much stronger than the initial re-normalization thanks to the magnetic dipole moment alone.

To aggregate the possible values that are attainable, we identify in Fig. 4(a) the maximum possible values of the magnetic enhancement inside the lattice as a function of the Mie angle that parametrizes the magnetic dipole Mie coefficient and the normalized periodicity. Here, we have systematically scanned the Mie angle that parametrizes the electric quadrupole moment and have chosen the value that maximizes the magnetic dipole moment. The required Mie angle for the electric quadrupole Mie coefficient that maximizes the magnetic dipole moment is shown in Fig. 4(b). This systematic analysis was greatly simplified by the availability of analytical expressions for the induced moments in the lattice.

Moreover, in Fig. 5 we have identified the set of Mie angles that provide the largest enhancement in the magnetic dipole moment for a suitably chosen period but above 100. Interestingly, we notice that the intrinsic magnetic dipole moment can take values below the resonance (negative Mie angle θ_{M1}) or above the resonance (positive Mie angle θ_{M1}) to achieve such colossal enhancement. Thanks to the interaction with the electric quadrupole moment, the re-normalization is always strong enough to enhance the magnetic dipole moment significantly. The electric quadrupole moment, in contrast, has to take always values below its resonance frequency to intensify the interaction; we observe only negative Mie angles.

We know the Mie coefficients that a particular particle should offer to provide a colossal magnetic dipole moment when placed on the lattice from these analytical considerations. However, the question is, always, whether we can suggest an actual particle that provides this response. To answer this question, we have been using a particle swarm optimization (PSO) algorithm that identifies a core-shell particle that can cope with these requirements and, indeed, we find such particle. The magnetic dipole moment as a function of the periodicity for such an optimized particle is shown in Fig. 6. Please note, other particles can be
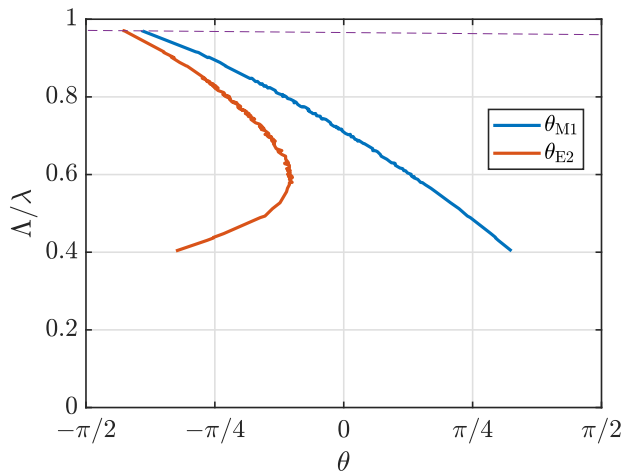
Fig. 5. The required Mie angles that parametrize the magnetic dipole and electric quadrupole Mie coefficients that allow to enhance the induced magnetic dipole moment for the normalized periodicity Λ/λ with two orders of magnitude. The dashed line in the figure indicates the chosen periodicity and the two Mie angles that in the subsequent search of an actual particle were used to provide these optical properties.

Fig. 6. Magnetic dipole moment of a designed core-shell particle when placed inside a lattice that shows an enhancement by more than two orders of magnitude in comparison to the maximal value an isolated scatterer can attain. The parameters of the core-shell particle are: $r_1 = 0.12350\lambda$, $r_2 = 0.20323\lambda$, $n_1 = 6$, $n_2 = 2.968$. The Mie coefficients are: $b1 = 0.1129 - 0.3165i$, $a2 = 0.0488 - 0.2155i$, $a1 = 0.4876 - 0.4998i$, $b2 = 0.0003 + 0.0180i$, $a3 = 0.0000 - 0.0035i$, $b3 = 0.0000 - 0.0014i$. The wavelength of illumination here is $\lambda = 1500$ nm.

found, depending on the Mie angles chosen as the target values. This example should merely provide a clear indication that there are actual particles that provide such desired response. Although other geometrical shapes might be feasible, we have been concentrating on a core-shell spherical particle for simplicity. The geometrical as well as the material properties that are necessary to provide the desired Mie angles and with that the colossal enhancement of the magnetic dipole moment are mentioned in the Fig. 6 caption. An enhancement as large as 100 with respect to the maximal possible value achievable in an isolated particle can be seen (i.e., in a non-absorbing magnetic dipole at resonance). This requires hitting a relatively sweet spot in terms of lattice dimensions.

Finally, we stress that other multipole moments have not been considered in the actual optimization. Of course, for the final particles, they are also non-zero and indicated up to quadrupolar order in the Fig. 6 caption. Their exact value is not crucial as the lattice anyhow is tuned into a regime where predominantly the magnetic dipole moment is enhanced. In parallel, the electric quadrupole moment is enhanced as well, as the denominator that expresses their re-normalization and which is brought close to zero is indeed identical.

5. CONCLUSIONS AND OUTLOOK

In a short conclusion, we have studied the extent to which the interaction among particles in a 2D lattice can enhance the induced magnetic dipole moment. We found an enhancement larger than 100 for an actual particle, which seems to justify the notion of "colossal". We emphasize that this is not the enhancement with respect to the magnetic dipole moment of the isolated object but to the magnetic dipole moment that is maximally feasible for an isolated scatterer. Interestingly enough, nearly any intrinsic magnetic dipole moment can be enhanced to provide an extremely large value, if only a suitable periodicity and electric quadrupole moment is chosen for the particle.

The work highlights the importance of lattice effects in nanophotonics. Very often, they are considered as a minor effect but indeed, as shown here, they can also have an overwhelming impact. This can be detrimental, for example, when considering metasurfaces made from scatterers with spatially varying geometrical shapes [64]. Still, it can also be appealing when the desire is to tweak the induced multipole moments in some sample to the desired combination unattainable with materials and objects at hand. Then, putting them in a lattice and exploiting the interaction can be decisive to reach the final goal.

The work also highlights the importance of analytical expressions for the optical properties of these arrays. Only with their availability, a systematic identification of scatterers with relevant properties is possible. The question of how an actual scatterer should look like that provides the desired response is a secondary task. That can be solved with many different tools [65], and here we have been using particle swarm optimization. More sophisticated tools can also be used to identify particles that provide the proper response individually and are also feasible for fabrication with some predefined materials or less sensitive to imperfections. These indications shall only highlight a few possibilities to develop the topic further.

Disclosures. The authors declare no conflicts of interest.

Data availability. Data underlying the results presented in this paper are not publicly available at this time but may be obtained from the authors upon reasonable request.

REFERENCES

1. K. M. Ho, C. T. Chan, and C. M. Soukoulis, "Existence of a photonic gap in periodic dielectric structures," Phys. Rev. Lett. **65**, 3152–3155 (1990).
2. S. Linden, C. Enrich, M. Wegener, J. Zhou, T. Koschny, and C. M. Soukoulis, "Magnetic response of metamaterials at 100 terahertz," Science **306**, 1351–1353 (2004).
3. C. M. Soukoulis and M. Wegener, "Past achievements and future challenges in the development of three-dimensional photonic metamaterials," Nat. Phot. **5**, 523–530 (2011).
4. E. N. Economou, "Surface plasmons in thin films," Phys. Rev. **182**, 539–554 (1969).
5. W. L. Barnes, A. Dereux, and T. W. Ebbesen, "Surface plasmon subwavelength optics." Nature **424**, 824–830 (2003).
6. G. Perrakis, O. Tsilipakos, G. Kenanakis, M. Kafesaki, C. M. Soukoulis, and E. N. Economou, "Perfect optical absorption with nanostructured metal films: design and experimental demonstration," Opt. Express **27**, 6842–6850 (2019).
7. E. Yablonovitch, "Inhibited spontaneous emission in solid-state physics and electronics," Phys. Rev. Lett. **58**, 2059–2062 (1987).
8. S. John, "Strong localization of photons in certain disordered dielectric superlattices," Phys. Rev. Lett. **58**, 2486–2489 (1987).
9. K. Sakoda, *Optical properties of photonic crystals*, vol. 80 (Springer Science & Business Media, 2004).
10. J. D. Joannopoulos, S. G. Johnson, J. N. Winn, and R. D. Meade, *Photonic crystals* (Princeton university press, 2011).
11. C. M. Soukoulis, *Photonic band gap materials*, vol. 315 (Springer Science & Business Media, 2012).
12. E. Cubukcu, K. Aydin, E. Ozbay, S. Foteinopoulou, and C. M. Soukoulis, "Negative refraction by photonic crystals," Nature **423**, 604–605 (2003).
13. D. R. Smith, S. Schultz, P. Markoš, and C. M. Soukoulis, "Determination of effective permittivity and permeability of metamaterials from reflection and transmission coefficients," Phys. Rev. B **65**, 195104 (2002).
14. N. Engheta and R. W. Ziolkowski, *Metamaterials: physics and engineering explorations* (John Wiley & Sons, 2006).
15. C. M. Soukoulis, S. Linden, and M. Wegener, "Negative refractive index at optical wavelengths," Science **315**, 47–49 (2007).
16. C. Chan, S. Datta, K. Ho, and C. Soukoulis, "Periodic dielectric structures: The long wavelength effective dielectric constant," in *Photonic Band Gaps and Localization,* (Springer, 1993), pp. 299–304.
17. P. Lalanne and D. Lemercier-lalanne, "On the effective medium theory of subwavelength periodic structures," J. Mod. Opt. **43**, 2063–2085 (1996).
18. I. V. Lindell, A. Sihvola, A. Viitanen, and S. Tretyakov, *Electromagnetic waves in chiral and bi-isotropic media* (Artech House on Demand, 1994).
19. C. Simovski, S. Tretyakov, A. Sochava, B. Sauviac, F. Mariotte, and T. Kharina, "Antenna model for conductive omega particles," J. Electromagn. Waves Appl. **11**, 1509–1530 (1997).
20. A. Serdyukov, I. Semchenko, S. Tretyakov, and A. Sihvola, *Electromagnetics of Bianisotropic Particles* (Gordon and Breach Science Publichers, 2001).
21. R. Alaee, M. Albooyeh, A. Rahimzadegan, M. S. Mirmoosa, Y. S. Kivshar, and C. Rockstuhl, "All-dielectric reciprocal bianisotropic nanoparticles," Phys. Rev. B **92**, 245130 (2015).
22. R. Alaee, M. Albooyeh, M. Yazdi, N. Komjani, C. Simovski, F. Lederer, and C. Rockstuhl, "Magnetoelectric coupling in nonidentical plasmonic nanoparticles: Theory and applications," Phys. Rev. B **91**, 115119 (2015).
23. V. S. Asadchy, A. Díaz-Rubio, and S. A. Tretyakov, "Bianisotropic metasurfaces: physics and applications," Nanophotonics **7**, 1069–1094 (2018).
24. V. G. Veselago, "Electrodynamics of substances with simultaneously negative and," Usp. Fiz. Nauk **92**, 517 (1967).
25. J. B. Pendry, "Negative refraction makes a perfect lens," Phys. Rev. Lett. **85**, 3966 (2000).
26. D. Schurig, J. J. Mock, B. Justice, S. A. Cummer, J. B. Pendry, A. F. Starr, and D. R. Smith, "Metamaterial electromagnetic cloak at microwave frequencies," Science **314**, 977–980 (2006).
27. U. Leonhardt and T. Tyc, "Broadband invisibility by non-euclidean cloaking," Science **323**, 110–112 (2009).
28. R. S. Penciu, K. Aydin, M. Kafesaki, T. Koschny, E. Ozbay, E. N. Economou, and C. M. Soukoulis, "Multi-gap individual and coupled split-ring resonator structures," Opt. Express **16**, 18131–18144 (2008).
29. K. Aydin, I. Bulu, K. Guven, M. Kafesaki, C. M. Soukoulis, and E. Ozbay, "Investigation of magnetic resonances for different split-ring resonator parameters and designs," New J. Phys. **7**, 168–168 (2005).
30. R. A. Shelby, D. R. Smith, and S. Schultz, "Experimental verification of a negative index of refraction," Science **292**, 77–79 (2001).
31. J. Zhou, T. Koschny, M. Kafesaki, E. N. Economou, J. B. Pendry, and C. M. Soukoulis, "Saturation of the magnetic response of split-ring resonators at optical frequencies," Phys. Rev. Lett. **95**, 223902 (2005).
32. C. Menzel, R. Alaee, E. Pshenay-Severin, C. Helgert, A. Chipouline, C. Rockstuhl, T. Pertsch, and F. Lederer, "Genuine effectively biaxial left-handed metamaterials due to extreme coupling," Opt. Lett. **37**, 596–598 (2012).
33. R. Alaee, C. Menzel, U. Huebner, E. Pshenay-Severin, S. Bin Hasan, T. Pertsch, C. Rockstuhl, and F. Lederer, "Deep-subwavelength plasmonic nanoresonators exploiting extreme coupling," Nano Lett. **13**, 3482–3486 (2013).
34. R. Marqués, F. Mesa, J. Martel, and F. Medina, "Comparative analysis of edge-and broadside-coupled split ring resonators for metamaterial design-theory and experiments," IEEE Trans. Antennas Propag. **51**, 2572–2581 (2003).
35. H. Chen, L.-X. Ran, J. T. Huang-Fu, X.-M. Zhang, K. S. Chen, T. M. Grzegorczyk, and J. A. Kong, "Magnetic properties of s-shaped split-ring resonators," Prog. In Electromagn. Res. **51**, 231–247 (2005).
36. G. Dolling, C. Enrich, M. Wegener, J. Zhou, C. M. Soukoulis, and S. Linden, "Cut-wire pairs and plate pairs as magnetic atoms for optical metamaterials," Opt. Lett. **30**, 3198–3200 (2005).
37. N. Yu and F. Capasso, "Flat optics with designer metasurfaces," Nat. Mat. **13**, 139–150 (2014).
38. A. I. Kuznetsov, A. E. Miroshnichenko, Y. H. Fu, J. Zhang, and B. Luk'Yanchuk, "Magnetic light," Sci. Reports **2**, 492 (2012).
39. A. V. Kildishev, A. Boltasseva, and V. M. Shalaev, "Planar photonics with metasurfaces," Science **339**, 1289 (2013).
40. A. Jain, P. Moitra, T. Koschny, J. Valentine, and C. M. Soukoulis, "Electric and magnetic response in dielectric dark states for low loss subwavelength optical meta atoms," Adv. Opt. Mater. **3**, 1431–1438 (2015).
41. M. Kerker, D.-S. Wang, and C. L. Giles, "Electromagnetic scattering by magnetic spheres," J. Opt. Soc. Am. **73**, 765–767 (1983).
42. R. Alaee, R. Filter, D. Lehr, F. Lederer, and C. Rockstuhl, "A generalized Kerker condition for highly directive nanoantennas," Opt. Lett. **40**, 2645–2648 (2015).
43. R. Dezert, P. Richetti, and A. Baron, "Complete multipolar description of reflection and transmission across a metasurface for perfect absorption of light," Opt. express **27**, 26317–26330 (2019).
44. R. Dezert, P. Richetti, and A. Baron, "Isotropic huygens dipoles and multipoles with colloidal particles," Phys. Rev. B **96**, 180201 (2017).
45. A. Epstein and G. V. Eleftheriades, "Huygens' metasurfaces via the equivalence principle: design and applications," J. Opt. Soc. Am. B **33**, A31–A50 (2016).
46. W. Liu and Y. S. Kivshar, "Generalized kerker effects in nanophotonics and meta-optics," Opt. Express **26**, 13085–13105 (2018).
47. A. Rahimzadegan, D. Arslan, D. Dams, A. Groner, X. Garcia-Santiago, R. Alaee, I. Fernandez-Corbaton, T. Pertsch, I. Staude, and C. Rockstuhl, "Beyond dipolar huygens' metasurfaces for full-phase coverage

and unity transmittance," Nanophotonics **9**, 75–82 (2020).

48. A. B. Evlyukhin, C. Reinhardt, U. Zywietz, and B. N. Chichkov, "Collective resonances in metal nanoparticle arrays with dipole-quadrupole interactions," Phys. Rev. B **85**, 245411 (2012).

49. V. E. Babicheva and J. V. Moloney, "Lattice effect influence on the electric and magnetic dipole resonance overlap in a disk array," Nanophotonics **7**, 1663–1668 (2018).

50. V. E. Babicheva and A. B. Evlyukhin, "Metasurfaces with electric quadrupole and magnetic dipole resonant coupling," ACS Photonics **5**, 2022–2033 (2018).

51. K. Y. Lee and M. A. El-Sharkawi, *Modern heuristic optimization techniques: theory and applications to power systems*, vol. 39 (John Wiley & Sons, 2008).

52. V. E. Babicheva and A. B. Evlyukhin, "Analytical model of resonant electromagnetic dipole-quadrupole coupling in nanoparticle arrays," Phys. Rev. B **99**, 195444 (2019).

53. J. D. Jackson, *Classical Electrodynamics* (Wiley, 1999).

54. A. Rahimzadegan, T. Karamanos, R. Alaee, A. G. Lamprianidis, D. Beutel, R. W. Boyd, and C. Rockstuhl, "A comprehensive multipolar theory for periodic metasurfaces," In preparation.

55. F. Bernal Arango, T. Coenen, and A. F. Koenderink, "Underpinning hybridization intuition for complex nanoantennas by magnetoelectric quadrupolar polarizability retrieval," ACS Photonics **1**, 444–453 (2014).

56. J. Mun, S. So, J. Jang, and J. Rho, "Describing meta-atoms using the exact higher-order polarizability tensors," ACS Photonics **7**, 1153–1162 (2020).

57. S. Tretyakov, *Analytical Modeling in Applied Electromagnetics* (Artech House, 2003).

58. D. Beutel, A. Groner, C. Rockstuhl, and I. Fernandez-Corbaton, "Efficient simulation of biperiodic, layered structures based on the t-matrix method," J. Opt. Soc. Am. B **38**, 1782–1791 (2021).

59. A. I. Dimitriadis, D. L. Sounas, N. V. Kantartzis, C. Caloz, and T. D. Tsiboukis, "Surface susceptibility bianisotropic matrix model for periodic metasurfaces of uniaxially mono-anisotropic scatterers under oblique te-wave incidence," IEEE Trans. Antennas Propag. **60**, 5753–5767 (2012).

60. I. Fernandez-Corbaton, S. Nanz, R. Alaee, and C. Rockstuhl, "Exact dipolar moments of a localized electric current distribution," Opt. Express **23**, 33044–33064 (2015).

61. H. C. Hulst and H. C. van de Hulst, *Light scattering by small particles* (Courier Corporation, 1981).

62. R. Gómez-Medina, P. San José, A. García-Martín, M. Lester, M. Nieto-Vesperinas, and J. Sáenz, "Resonant radiation pressure on neutral particles in a waveguide," Phys. Rev. Lett. **86**, 4275 (2001).

63. A. Rahimzadegan, R. Alaee, C. Rockstuhl, and R. W. Boyd, "Minimalist mie coefficient model," Opt. Express **28**, 16511–16525 (2020).

64. C. Gigli, Q. Li, P. Chavel, G. Leo, M. Brongersma, and P. Lalanne, "Fundamental limitations of huygens' metasurfaces for optical beam shaping," arXiv e-prints pp. arXiv–2011 (2020).

65. T. Wu, A. Baron, P. Lalanne, and K. Vynck, "Intrinsic multipolar contents of nanoresonators for tailored scattering," Phys. Rev. A **101**, 011803 (2020).